



Lasers in Manufacturing Conference 2023

Quality and safety monitoring of the laser beam welding process for battery module contacting using a multi-sensor concept

Michael Riesener^a, Maximilian Kuhn^a, Christian Höltgen^{a*}, Florian Kaufmann^b, Günther Schuh^a

^aLaboratory for Machine Tools and Production Engineering (WZL) of RWTH Aachen University, Campus Boulevard 30, 52074 Aachen, Germany

^bBayerisches Laserzentrum GmbH (blz), Konrad-Zuse-Straße 2-6, 91052 Erlangen, Germany

Abstract

One of the most relevant joining technologies for electromobility components is laser welding. High precision, contactless welding joints and flexible process design options enable high quality requirements to be met. In the field of battery systems, the weld seam quality of the cell connectors has a direct influence on the performance of the entire system. In addition, there is a risk of cell fire, which can be caused by faulty process conditions. The aspects of quality and safety monitoring therefore play a decisive role in the economic production of high-quality battery systems. Therefore, the aim of this work is to investigate a multi-sensor concept that monitors the quality-critical process parameters temperature and electrical resistance before, during, and after the welding process. Besides recording the sensor values, several test procedures were used to analyse the quality of the welding seams to compare them with the process parameters.

Keywords: Electromobility; Quality Monitoring; Safty Monitoring; Sensor; Welding

1. Introduction

The automotive industry has a decisive influence on the achievement of global climate goals. In the EU, road transport is responsible for one fifth of greenhouse gas emissions. At 61%, private cars account for the

* Corresponding author. Tel.: +49 241-802-1575; fax: +49-241-802-2293.
E-mail address: c.hoeltgen@wzl.rwth-aachen.de.

largest share [European Environment Agency]. The demand for electric vehicles has increased rapidly in recent years due to the importance of sustainable drive concepts as shown in Regulation (EU) 2019/631 of the European Parliament. As a result, electric vehicles are being produced in large numbers. Due to the increasing importance of electromobility, the materials copper and aluminium are being used in large numbers in drive and battery systems. Their high electrical and thermal conductivity predestine them for use in electricity conduction as well as heat dissipation. The advantages of a defined, local heat input in combination with high achievable process speeds and good automation have made laser welding an indispensable joining technology, especially in automotive production. The application of laser welding with the above-mentioned materials is difficult as the materials reflect a large amount of infrared laser radiation. This is a significant challenge, especially in the production of battery systems, where unstable joining processes not only have a negative impact on quality, but also cause the risk of a battery cell fire. The work by Günter, 2022 presents that lithium-ion cells are mainly used as energy storage for automotive battery systems. The welding process introduces thermal energy into the battery, especially to the cell conductors. This thermal stress can lead to ageing of the cell. The most thermally sensitive component of the cell is the electrolyte. Above a temperature of 65°C, decomposition reactions begin. This reduces the performance and the lifetime of the cell. To avoid negative influences of the welding process, the temperature at the cell conductors is not allowed to exceed the maximum temperature of 65°C as shown by Ravdel et al., 2003. The main task in the electrical contacting of battery cells is to create a joint which has the lowest possible electrical resistance. Aluminium-copper mixed joints with low electrical resistance are difficult to produce, due to the formation of intermetallic phases (IMP), which reduce the electrical properties of the weld, as well as due to the different melting points of aluminium and copper. Optical measuring methods, such as optical coherence tomography (OCT) or camera systems, offer the possibility to directly or indirectly evaluate the quality-critical parameters of temperature and electrical resistance as shown by Kang et al., 2022. Under real process conditions, however, large areas around the joint are covered by interfering elements or fixture and thereby may not be measured with optical methods. The integration of sensors in fixture elements can therefore be a possible solution.

2. Experimental setup

2.1. Material

This study uses aluminium AIN30 (Al) and nickel-plated copper (Cu) with a sheet thickness of 0.2 mm for the Cu and 0.3 mm for the Al plate. Both plates had a dimension of 55 mm in length and 35 mm in width. The plates were positioned in overlap configuration. The 2.5 µm thick Ni-coating on the Cu-ETP plates was electrodeposited, with a tolerance specified between 0.6 and 3 µm. The chemical composition of the materials is listed in Table 1 according to the supplier inspection sheet from Kunshan Huaiyuan Battery material Co., Ltd.

Table 1. Chemical composition of AIN30 and Ni-plated copper in wt. %

Material/Element	Al	Zn	Mg	Mn	Cu	Si + Fe
Al (AIN30)	99.42	0.01	0.01	0.01	0.01	0.47
Cu (Cu, 2.5 µm Ni-layer)	-	-	-	-	99.96	-

2.2. Welding Setup

The study were performed with a disk laser TruDisk 4001 (TRUMPF Laser GmbH + Co. KG, Ditzingen, Germany) emitting 4 kW maximum cw-out-put power at $\lambda = 1030$ nm wavelength. The laser beam is guided through a fiber-optic cable with a core diameter of $d_{LLK} = 100$ μm to the welding optics (PFO 3D). Optics with a focal length of 450mm are used. This optic enables a processing field size in the form of an ellipse of 320mm x 190mm. The copper and aluminium joints were processed in the focal plane at $z = 0$ mm (Al top surface). The properties of the laser source and the optical setup are listed in Table 2.

Table 2. Laser beam source and optical setup used for the investigation

Dimension	Unit	Trumpf TruDisk 4001
Wavelength (λ)	[nm]	1030
Laser power (P_{max})	[W]	4000
Fiber diameter (d_{LLK})	[μm]	100
Focal length collimator (f_c)	[mm]	138
Focal length optics (f_f)	[mm]	450
Focal diameter (d_f)	[μm]	350

The customized experimental setup for the investigation is based on the setup presented by Bergweiler et al., 2022, which was developed in cooperation with the Bayerisches Laserzentrum GmbH. A schematic sketch of the experimental setup is shown in Fig. 1.

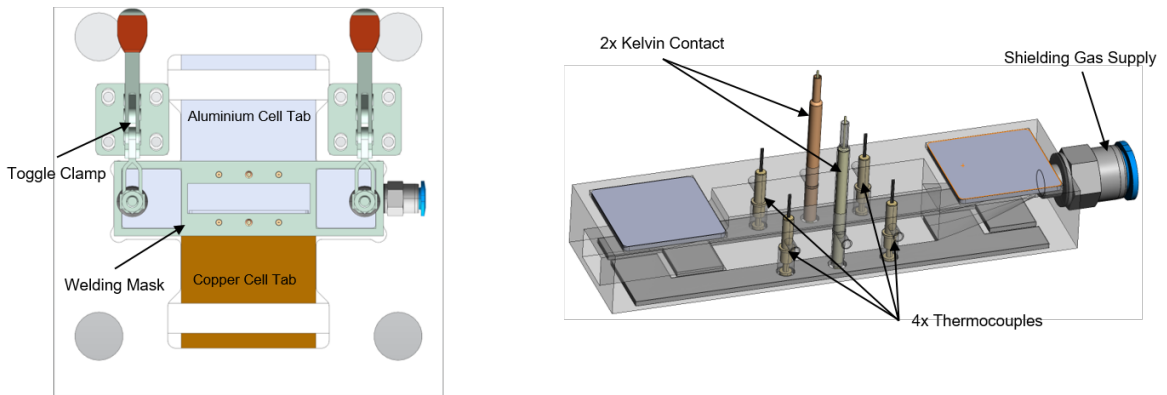


Fig. 1. (left) Clamping fixture with integrated sensor technology; (right) detailed view of the welding mask

The welding mask has the task of pressing the joining partners together to a technical zero gap. It is additively manufactured and integrates several functionalities. The contact surfaces and force application are reinforced with steel plates. The welding mask is pressed onto the joining partners by means of toggle clamps. As a component that has direct contact with the joining partners, the mask provides the optimal basis for the integration of various tactile measuring systems. In addition, the flexibility of additive manufacturing makes functionalities such as shielding gas supply possible. Argon is used as inert gas. The process gas pressure is 2 bar. The measurement setup is designed for the evaluation of the pre-, in-process and post-process data. The temperature measurement is the basis for the thermal evaluation of the welding parameters. The

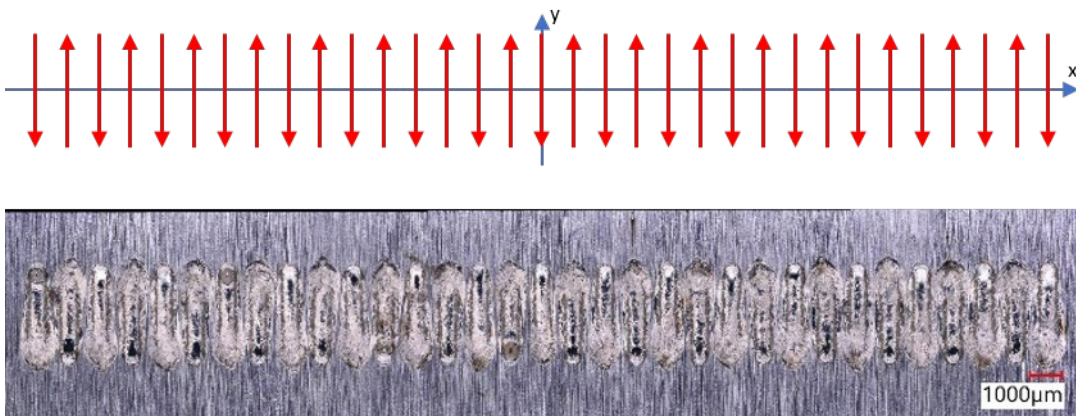
measurement records a temporal progression of the temperature on the cell tabs, with regard to the top and bottom plate (in-process). The thermocouples used in the study are type K sensors, which are suitable for temperatures up to 177°C. The temperature of the tabs is measured with type K sensors (brass, gold plated; UWE electronic GmbH, Unterhaching, Germany). The temperature of the traps are measured with 2 sensors each.

The integrated resistance measurement in the welding mask is used to continuously record process data, which can be used to derive various findings about the quality of the welded joint. With the measured values recorded before the welding process (pre-process), the correct positioning of the welding mask can be recognised, as the contact resistance of the unwelded sheets has a consistently high value. If the required zero gap is not created due to incorrect clamping of the sheets, this can be detected by a deviation of the resistance values. This can avoid the production of low-quality battery modules and reduce the risk of thermal runaway. The resistance values recorded after welding (post-process) are used as a measure of the quality of the joint. Negative effects on the electrical conductivity, such as intermetallic phases, can thus be detected. The electrical resistance measurement was executed by a combined measurement of the voltage and current as suggested by Ohm's law as shown by Hollatz et al., 2020. Therefore, a four-wire-measurement setup was built to introduce a defined current through the welded samples. For the measurement of the electrical resistance, two spring-loaded Kelvin contacts (UWE electronic GmbH, Germany) were integrated into the welding mask.

2.3. Experimental Design and Procedure

For the experimental investigations a linear stitched weld was examined. The linear stitched weld is characterized by single lines of $l = 3$ mm length. These single lines were arranged at a horizontal distance of 1 mm, welded in alternating y -direction. In order to symmetrically distribute the energy input, the first seam is placed at $x = 0$ mm in negative y -direction, followed by two seams at $x = -1$ mm and 1 mm in positive y -direction. This stitching was then repeated 15 more times in alternating y -direction (Figure 2).

Fig. 2. (top) Linear stitched weld; (bottom) image of the weld seam



A total amount of 350 Cu and Al plate pairs was available for the investigation of the seam properties of overlap welding strategies from copper to aluminium in this work. In preliminary tests, process parameters were developed which ensure good connection quality, assessed first by visual inspection of the generated weld seams and followed by metallographic analysis. If no connection in the overlapping area or if an excessive energy input was achieved (weld seam completely penetrates the Cu-sample), the process parameters laser

power and feed rate (or frequency respectively for oscillation strategies) were subsequently carefully adjusted. The center point settings for the welding strategy was developed with a laser power of 2500 W and a feed rate of 550 mm/s. The parameter set was also tested for reproducibility, with the parameter set welded at least 10 times. During the welding process, the temperature and the electrical resistance were continuously recorded.

3. Results and Discussion

3.1. Temperature Measurement

In Fig.3, the temporal temperatures occurring in the seam adjacent zone during the welding process are shown. All measured temperatures in the seam adjacent zone were below the maximum permissible temperature of $T_{crit} = 65 \text{ }^{\circ}\text{C}$. At a distance of 8 mm between the symmetry plane of the weld seam and the measuring points, a maximum temperature of $52 \text{ }^{\circ}\text{C}$ was detected on the aluminium tab side. In general, the maximum temperature was recorded in the aluminium sheet, as can be seen, for instance, in the diagram in Figure 3 which was attributed to the upper positioning. Since the welding process takes only about one second of time, a rapid heating of the welded samples takes place, followed by different cooling curves for both metals. This high thermal gradient favors the formation of intermetallic phases in the weld seam area as shown by Lei et al., 2021, but also leads to the fact that the seam adjacent zones stayed below T_{crit} .

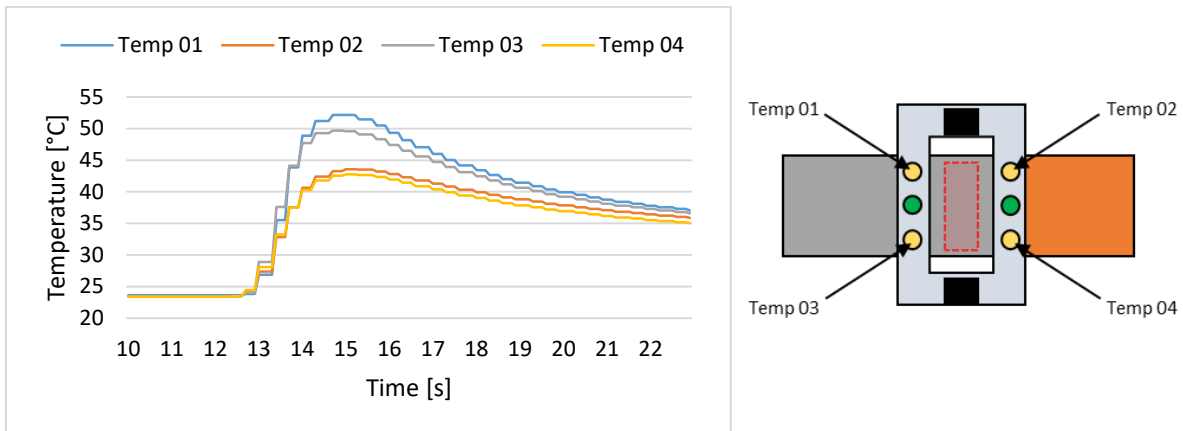


Fig. 3. (left) In-line measurement of the temperature; (right) position of the sensors in the welding mask

Based on the measurement results, it is recommended for the application of laser-based contacting of battery tab connections to ensure a minimum distance of 20 mm between the center of the weld trajectory and the critical component (e.g., the current collector edge).

3.2. Electrical Connection Resistance

Fig. 4 shows the results for the electrical connection resistance measurement of a welded joint. As can be seen on the right side of the graph, a constant resistance can be measured before the actual welding process. In the series of tests carried out here, values between $180 - 220 \mu\Omega$ were measured before the welding process. Evaluations regarding a dependency between the variance of the initial resistance and the achieved quality of the weld seam could not be derived in the study results. At the beginning of the welding process, which can

be seen in Fig. 4 as the curve is segregated during process, is a short-term deflection of the measured values. This allows the temporal start of the welding to be detected via the measured values of the electrical resistance. During the welding process, no evaluable measured values can be recorded. After the welding process, a time-dependent change in the electrical resistance is recorded. After a minimum ($20.8 \mu\Omega$) of the electrical resistance is recorded about one second after the welding process, the measured value increases to the value of $73.9 \mu\Omega$ by the end of the data recording. This can be related to the formation of intermetallic phases and the temperature change of the materials after the welding process. A more detailed investigation of the connection was not carried out within the scope of this study.

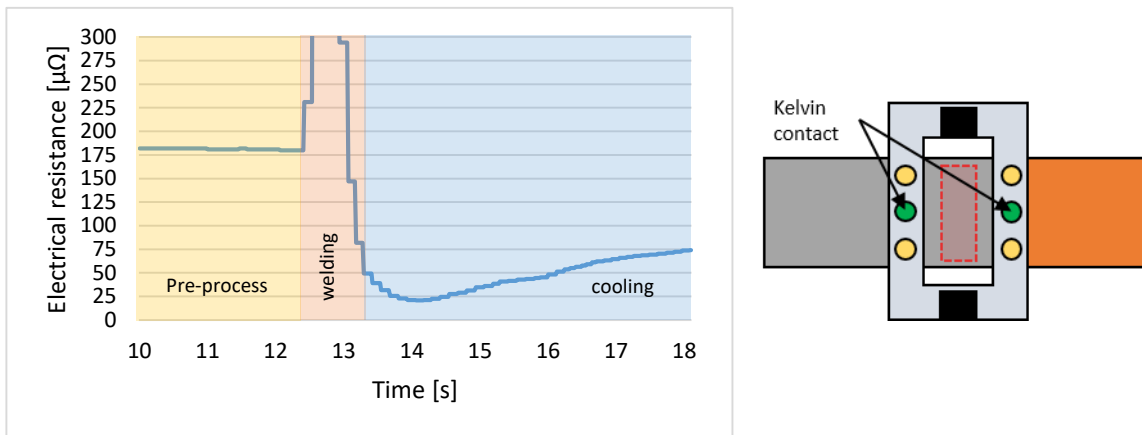


Fig. 4. (left) In-line measurement of the electrical resistance; (right) position of the sensors in the welding mask

3.3. Discussion

The measured values of temperature and electrical resistance shown here demonstrate that it is possible to monitor the joining process of batteries with tactile sensors that are located in a welding fixture. The direct measured values of temperature and electrical resistance can provide direct information about the quality of the joint during the process. A more precise analysis of the temporal course of the measured values can provide further information and help to analyse the weld seam. However, this requires further tests to generate a larger database that can be used to establish more precise correlations between the in-process measured values and the subsequent results of metallurgical and mechanical investigations. The samples produced in this study were analysed in more detail by carrying out tensile-shear strength tests and the evaluation of weld seam cross-sections, among other tests. For a detailed metallurgical and mechanical characterisation of the same sample geometry using a laser beam source in the green spectral range, please refer to the publication by Kaufmann et al, 2023.

4. Outlook

In order to be able to provide better information about the quality of the weld seam by means of the recorded data, further evaluation of the collected data and the execution of further tests is necessary. Here, the combination with optical measuring systems such as OCT or thermographic cameras must also be taken into account in order to be able to generate an extensive database. It must always be taken into account that the integration of further sensor technology into the fixture should not hinder the main function of the fixture,

which is clamping the joining partners. Furthermore, the developed fixture and sensor system must be further developed in order to be able to clamp and monitor joints of different battery formats. With a better understanding of the measurement results, detailed predictions about the condition of a battery system after the manufacturing stage can be made. This is an important component for the creation of a digital product passport. This enables better planning of the further Life Cycles of the product, which leads to a sustainable use of batteries in the long term.

References

- European Environment Agency, 2022, National Emissions Reported to the UNFCCC and to the EU Greenhouse Gas Monitoring Mechanism.
- Regulation (EU) 2019/631 of the European Parliament and of the Council of 17 April 2019 Setting CO₂ Emission Performance Standards for New Passenger Cars and for New Light Commercial Vehicles, and Repealing Regulations (EC) No 443/2009 and (EU) No 510/2011.
- Günter, F.J., Wassiliadis, N., 2022, State of the Art of Lithium-Ion Pouch Cells in Automotive Applications: Cell Teardown and Characterization, *Journal of The Electrochemical Society*.
- Ravdel, B., Abraham, K., Gitzendanner, R., DiCarlo, J., Lucht, B., Campion, C., 2003, Thermal stability of lithium-ion battery electrolytes, *Journal of Power Sources* 119-121, p. 805-810
- Kang, S., Kang, M., Jang, Y. H., Kim, C., 2022, Deep learning-based penetration depth prediction in Al/Cu laser welding using spectrometer signal and CCD image, *Journal of Laser Applications* 34.
- Bergweiler, G., Höltgen, C., Kaufmann, F., Fiedler, F., 2022, Elektromobilproduktion mittels grüner Multi-kW-Laserbearbeitung, *Maschinenbau* 2, p.36–40.
- Hollatz, S., Kremer, S., Ünlübayir, C., Sauer, D.U., Olowinsky, A., Gillner, A., 2020, Electrical Modelling and Investigation of Laser Beam Welded Joints for Lithium-Ion Batteries, *Batteries* 6.
- Lei, Z., Zhang, X., Liu, J., Li, P., 2021, Interfacial microstructure and reaction mechanism with various weld fillers on laser welding/brazing of Al/Cu lap joint, *Journal of Manufacturing Processes*, 67, p. 226-240.
- Kaufmann, F., Strugulea, M., Höltgen, C., Rotth, S., Schmidt, M., 2023, Seam Properties of Overlap Welding Strategies from Copper to Aluminum Using Green Laser Radiation for Battery Tab Connections in Electric Vehicles, *Materials* 16, 1069.